The subcortical and neurochemical organization of the ventral and dorsal attention networks

Pedro Nascimento Alves, Stephanie Forkel, Maurizio Corbetta, Michel Thiebaut de Schotten

The subcortical and neurochemical organization of the ventral and dorsal attention networks

Alves PN [1,2*]; Forkel SJ [3-6]; Corbetta M [7-10], Thiebaut de Schotten M [3,11].

[1] Laboratório de Estudos de Linguagem, Centro de Estudos Egas Moniz, Faculdade de Medicina, Universidade de Lisboa, Lisboa, Portugal

[2] Serviço de Neurologia, Departmento de Neurociências e Saúde Mental, Hospital de Santa Maria, CHULN, Lisboa, Portugal

[3] Brain Connectivity and Behaviour Laboratory, Sorbonne University, Paris, France

[4] Donders Institute for Brain Cognition Behaviour, Radboud University, Thomas van Aquinostraat 4, 6525GD Nijmegen, the Netherlands

[5] Centre for Neuroimaging Sciences, Department of Neuroimaging, Institute of Psychiatry, Psychology and Neuroscience, King's College London, London, UK

[6] Departments of Neurosurgery, Technical University of Munich School of Medicine, Munich, Germany.

[7] Clinica Neurologica, Department of Neuroscience, University of Padova, Italy

[8] Padova Neuroscience Center (PNC), University of Padova, Italy

[9] Venetian Institute of Molecular Medicine, VIMM, Padova, Italy

[10] Department of Neurology, Radiology, Neuroscience Washington University School of Medicine, St.Louis, MO, USA

[11] Groupe d'Imagerie Neurofonctionnelle, Institut des Maladies Neurodégénératives-UMR 5293, CNRS, CEA, University of Bordeaux, Bordeaux, France

Abstract

Attention is a core cognitive function that filters and selects behaviourally relevant information in the environment. The cortical mapping of attentional systems identified two segregated networks that mediate stimulus-driven and goal-driven processes, the Ventral and the Dorsal Attention Networks (VAN, DAN). Deep brain electrophysiological recordings, behavioural data from phylogenetic distant species and observations from human brain pathologies challenge purely corticocentric models. Here, we used advanced methods of functional alignment applied to resting-state functional connectivity analyses to map the subcortical architecture of the Ventral and the Dorsal Attention Networks. Our investigations revealed the involvement of the pulvinar, the superior colliculi, the head of caudate nuclei, and a cluster of brainstem nuclei relevant for both networks. These nuclei are densely connected structural network hubs as revealed by diffusion-weighted imaging tractography. Their projections establish interrelations with the acetylcholine nicotinic receptor as well as dopamine and serotonin transporters, as demonstrated in a spatial correlation analysis with a normative atlas of neurotransmitter systems. This convergence of functional, structural, and neurochemical evidence provides a novel framework to comprehensively understand the neural basis of attention across different species and brain diseases.

Introduction

"Everyone knows what attention is. It is the taking possession by the mind, in clear and vivid form, of one out of what seem several simultaneously possible objects or trains of thought." (James 1890).

Everything we see, feel, or smell is an illusion elaborated by our brain circuits. However, the brain's capacity is limited. This requires mechanisms for the selection of the most relevant information. The ensemble of cognitive and neural processes involved in capacity limitation and selection underlies 'attention' as defined by James (1890). Behavioural studies have distinguished orienting of attention into a slow, strategic, goal-directed, and voluntary component versus a swift, unexpected, bottom-up, and automatic component (Posner 1980; Petersen and Posner 2012). Task-related functional neuroimaging (*f*MRI) studies segregated these two attentional processes anatomically into a dorsal and ventral attentional network (Corbetta and Shulman 2002, for a review). The Dorsal Attention Network (DAN) encodes and maintains preparatory signals and modulates top-down sensory (visual, auditory, somatosensory) regions.

In contrast, the Ventral Attention Network (VAN) is recruited when attention is re-oriented to novel behaviourally relevant events. Classical core regions of the DAN are the intraparietal sulcus, the superior parietal lobe, and the frontal eye fields. The DAN is considered to have no hemispheric lateralization (Corbetta et al. 2000, 2008; Buschman and Miller 2007; Thiebaut de Schotten et al. 2011a; Amemiya et al. 2021). In contrast, the temporo-parietal junction and the ventrolateral prefrontal cortex constitute the central regions of the VAN. Evidence demonstrates that the VAN is right lateralized (Downar et al. 2000; Corbetta et al. 2008; Thiebaut de Schotten et al. 2011a). Within their respective networks, DAN and VAN regions have synchronous

*f*MRI signal oscillations at rest (Fox et al. 2006; Corbetta et al. 2008; Power et al. 2011; Yeo et al. 2011; Vossel et al. 2012; Szczepanski et al. 2013; Gordon et al. 2016; Schaefer et al. 2018; Sani et al. 2021). Thanks to this synchronization, the two networks have consistently been identified and segregated in resting-state *f*MRI cortical parcellations (Power et al. 2011; Yeo et al. 2011; Gordon et al. 2016; Schaefer et al. 2018), although their taxonomy has not always been homogenous in the literature (Eickhoff et al. 2018; Uddin et al. 2019). Hence, the DAN and VAN are organized as independent networks even in the absence of task signals. However, their synchronization can change according to task demands, and they can be acting jointly or separately (Luo et al. 2010; Corbetta and Shulman 2011). Furthermore, DAN and VAN task activations and synchronization levels are modified by focal lesions and correlate with behavioral deficits (Corbetta et al. 2005; He et al. 2007; Ptak and Schnider 2010; Li et al. 2012; McCarthy et al. 2013; Baldassarre et al. 2014; Ramsey et al. 2016; Sanefuji et al. 2017).

Yet, electrical recording, pathological observations, and phylogenetic comparisons demonstrate that the neuroanatomical framework of attentional mechanisms should extend well beyond a corticocentric model. Electrical recordings in primates showed that subcortical structures have a crucial role in the neural mechanisms of attention. For instance, inactivation of the superior colliculus during motion-change detection markedly disturbs visual attention without affecting the neuronal activity in the visual cortex (Zénon and Krauzlis 2012). Attentional states also modulate the thalamic pulvinar nuclei (Bender and Youakim 2001; Saalmann and Kastner 2011) and neuronal discharge patterns in the locus coeruleus (Aston-Jones et al. 1999; Vazey et al. 2018). Pathophysiological data from human brain disease supports the critical relevance of deep brain nuclei. Neglect is a clinical syndrome characterized by

pathological hemispatial inattention (Bartolomeo 2013) and can arise from subcortical lesions in the pulvinar, striatum, or superior colliculus (Healton et al. 1982; Ferro et al. 1984; Karnath et al. 2002; Nyffeler et al. 2021). Patients with attention deficit hyperactivity disorder also present alterations beyond the cortex (Sanefuji et al. 2017), such as in the pulvinar, which is influenced by the severity of the disease and the use of stimulants (Ivanov et al. 2010).

Additionally, distant phylogenetic species, such as pigeons, have markedly different cortical morphologies but exhibit attention errors and reaction times similar to humans (Blough 1977). With close mammals, such as macaques, relevant functional attention dissimilarities have been described at the cortical level, including the complete absence of a VAN (Patel et al. 2015). Hence, a core phylogenetically relevant subcortical network of areas appears to support the orientation of attention that has been mostly disregarded in the functional neuroimaging literature because of limited field strength or issues arising from average group alignments. Average group alignments of functional neuroimaging maps exclusively based on structural landmarks might typically fail to represent an accurate functional network due to inter-individual differences (Brett et al. 2002; Thiebaut de Schotten and Shallice 2017). Specifically, subcortical nuclei are prone to structural misalignment due to their small size, poor contrast in structural MRI, and intersubject cytoarchitectonic variability (Carmack et al. 2004; Amunts et al. 2005, 2013; Zaborszky et al. 2008). In contrast, advanced methods of functional alignment improve structural-functional correspondence across participants (Mueller et al. 2013; Robinson et al. 2014; Langs et al. 2015; Glasser et al. 2016). Further, surface interindividual alignment based on morphological features, such as cortical folding, fairly aligns unimodal cortical areas, such as the primary visual and motor cortices, but poorly overlaps higher-order

cortical areas (Fischl et al. 2008; Mueller et al. 2013). Methods of functional alignment based on *f*MRI signals during cognitive activation paradigms (Sabuncu et al. 2010; Conroy et al. 2013) and resting-state *f*MRI connectivity patterns (Langs et al. 2015; Nenning et al. 2020) provided better function matching and have also been used for cross-species functional comparisons (Xu et al. 2020). Functional alignment is different from hyperalignment techniques that project shared neural information beyond the three-dimensional anatomical space, i.e., in high-dimensional spaces (Haxby et al. 2011, 2020; Guntupalli et al. 2016). At the subcortical level, our team also demonstrated that functional alignment methods can optimize the group-level mapping of functional networks, improving functional correlations and uncovering a network's deep brain nuclei components (Alves et al. 2019). However, this method has never been applied to explore the subcortical anatomy of the VAN and the DAN.

Delineating the subcortical components of the DAN and the VAN would allow us to revisit their underlying circuitry through diffusion-weighted imaging tractography that enables *in vivo* reconstruction of associative, commissural, and projection white matter tracts (Behrens et al. 2003; Catani and Thiebaut de Schotten 2012; Zhang et al. 2022). A clearer characterization of the DAN and VAN circuitry will help to better understand brain interactions in healthy and pathological brains (Suárez et al. 2020; Thiebaut de Schotten et al. 2020).

Subcortical structures also play a critical role within the neurotransmitter systems. Brainstem nuclei are the primary sources of neurotransmitter synthesis and send axonal projections to the cortex and the basal ganglia. The basal ganglia are central targets of the neurotransmitter axonal projections and mediate their physiological effects. Yet the neurochemistry of the DAN and the VAN is limited to primate studies. These studies reported a noradrenergic innervation of regions of the primate

attention networks, including the temporo-parietal junction and the frontal lobe (Morrison and Foote 1986; Foote and Morrison 1987; Bouret and Sara 2005). Noradrenaline has been proposed as a critical trigger for the reorientation of attention (Bouret and Sara 2005; Corbetta et al. 2008). However, despite its essential neuroscientific and medical importance (Sanefuji et al. 2017) the neurochemical signatures of the VAN and the DAN have never been contrasted in humans. Such an endeavor is now possible thanks to the macroscale mapping of the neurotransmitter receptors and transporters in humans by means of positron emission tomography (PET) and single-photon emission computerized tomography (SPECT) scans (Hansen et al. 2021). Accordingly, a normative atlas of nine neurotransmitter systems aligned in the MNI space is now openly available and allows for the first time for the investigation of the neurochemical signature of brain circuits.

Therefore, we explored the subcortical anatomy of attention networks by aligning the individual resting-state functional maps of the VAN and the DAN in a common functional space. Based on previous electrical recordings, pathological observations, and phylogenetic reports, we hypothesized that basal ganglia and brainstem nuclei, namely the pulvinar, the striatum, the superior colliculi, and the locus coeruleus, are core phylogenetically relevant and functional constituents of the attention networks. Finally, an optimized model of the VAN and the DAN was proposed together with their structural, functional, graph centrality, and neurochemical signature.

Methods

Resting-state functional imaging (rs-*f*MRI)

We used 110 7T resting-state functional MRI datasets from the Human Connectome Project S1200 (Glasser et al. 2013). Images were preprocessed and

registered to the MNI152 space as specified in the Human Connectome Project protocol (http://www.humanconnectome.org/storage/app/media/documentation/s1200/HCP_S1200_Release_Reference_Manual.pdf; Glasser et al. 2013).

VAN and DAN maps in the structural space

VAN and DAN maps were computed using seed regions of interest defined in the functional cortical parcellation map (Gordon et al. 2016). This template includes 23 VAN parcels (11 in the left and 12 in the right hemisphere) and 32 DAN parcels (19 in the left and 13 in the right hemisphere). This parcellation was performed according to resting-state functional connectivity patterns. Each parcel has a homogeneous resting-state functional connectivity signature and is separated from neighboring parcels by abrupt changes in their connectivity profile (Gordon et al. 2016).

We calculated functional correlation maps seeded from each VAN cortical parcel using the Funcon-Connectivity tool implemented in the Brain Connectivity and Behaviour toolkit (http://toolkit.bcblab.com; Foulon et al. 2018). This tool computes Pearson's correlation between a seed region's mean resting-state activity and the brain's other voxels. Then, the median of the 23 functional connectivity maps (generated from the 23 VAN seeds) was computed to obtain the VAN's most representative map for each participant. We chose a median because it is less affected by outliers than the mean (Kenney 1939). 110 individual VAN maps in the MNI152 were obtained (i.e. one per subject). The same steps were performed to obtain 32 DAN maps.

VAN and DAN maps in the functional space

The 110 individual VAN Pearson's correlation maps in the MNI152 space were aligned in a functional space to optimize their inter-individual alignment of functional areas (Mueller et al. 2013; Robinson et al. 2014; Langs et al. 2015; Glasser et al. 2016). We used the Advanced Normalization Tools (ANTs) script 'buildtemplateparallel.sh' to perform an iterative (n=4) diffeomorphic transformation to a common space (Avants et al. 2011; Alves et al. 2019). Cross-correlation was set as the similarity measure and greedy SyN as the transformation model (Avants et al. 2008; Klein et al. 2009). The resulting transformation warps were applied to the MNI152 aligned VAN maps, using the ANTs' script 'WarpImageMultiTransform' to represent the 110 individual VAN maps in the functional space. The same steps were performed with the 110 DAN Pearson's correlations maps. A schematic representation of the functional alignment steps is available in Supplementary Figure 1.

To calculate group statistical VAN and DAN maps, we performed a permutation inference analysis using FSL's 'randomise' one-sample (5000 permutations) and applied a Threshold-Free Cluster Enhancement (Jenkinson et al. 2012). To evaluate the similarity between the VAN and DAN statistical maps, the t-maps were z-transformed, and a conjunction analysis was computed (Nichols et al. 2005). A difference map was also calculated by subtracting the median DAN Pearson's correlation map from the VAN. Illustrations were produced in SurfIce (https://www.nitrc.org/projects/surfice/) and MRIcroGL (https://www.nitrc.org/projects/mricrogl/).

Anatomical validation of the subcortical structures

To identify thalamic nuclei, we visually compared our results with the DISTAL (Deep brain stimulation Intrinsic Template Atlas; Ewert et al. 2018) and the THOMAS (Thalamus Optimized Multi Atlas Segmentation; Su et al. 2019) atlases. The DISTAL atlas is a high-resolution template of subcortical structures in the MNI space used as a reference to localize targets for deep brain stimulation (Ewert et al. 2018). The DISTAL atlas segmentation was performed manually, based on histology, structural imaging, and diffusion-weighted imaging (Chakravarty et al. 2006; Ewert et al. 2018). The THOMAS atlas is a template of thalamic nuclei derived from the manual segmentation of 20 White-Matter-Nulled Magnetization Prepared Rapid Gradient Echo (MP-RAGE) 7T datasets warped to the MNI space (Su et al. 2019). We used the WIKIBrainStem atlas to identify the brainstem nuclei (Lechanoine et al. 2021). This template is based on mesoscopic T2-weighted and diffusion-weighted images obtained from the ultra-high-field scanning (11.7T) of an *ex vivo* human specimen. It provides detailed segmentations of 99 brainstem structures (Lechanoine et al. 2021).

Tractography analysis

We analyzed the structural connectivity of the VAN and DAN, including the new subcortical structures identified in our resting-state functional connectivity analysis. Tractography was computed using 177 diffusion-weighted images from the 7T dataset of the Human Connectome Project (Vu et al. 2015). The scanning parameters are detailed in Vu et al. 2015. Preprocessing was performed according to the default Human Connectome Project pipeline (v3.19.0; Glasser et al. 2013). Tractography processing was prepared as described in Thiebaut de Schotten et al. 2020 (available at http://opendata.bcblab.com). Briefly, a whole-brain deterministic algorithm was

employed using StarTrack (https://mr-startrack.com) applying a damped Richardson-Lucy algorithm optimized for spherical deconvolution (Dell'Acqua et al. 2010). Then, the individual whole-brain streamline tractograms were registered to the MNI152 space. First, they were converted into density maps, in which the voxel densities corresponded to the number of streamlines crossing each voxel (Thiebaut de Schotten et al. 2020). Second, individual density maps were aligned to a standard template using the Greedy symmetric diffeomorphic normalization of the Advanced Normalization Tools pipeline (Avants et al. 2011). Third, the resulting template was co-registered to the MNI152 2mm template using the FSL's tool 'flirt' (Jenkinson et al. 2002). Finally, the resulting transformation warps were applied to the individual whole-brain streamline tractography using Tract Querier (Wassermann et al. 2016).

Then, we computed the structural connectome of the VAN and DAN models. The cortical nodes were defined according to Gordon et al. 2016. To determine the subcortical regions of interest, we selected the statistically significant voxels of the subcortical structures identified in the previous sections with a median Pearson's correlation above r=0.1. This correlation threshold was applied to avoid including voxels significantly associated with the network but with weak correlations (Cohen 1988). The streamlines that crossed at least two ROIs (cortico-cortical, cortico-subcortical, or subcortical-subcortical) were selected using the MRtrix3's tool 'tckedit' (Tournier et al. 2019). Afterwards, the selected streamlines were converted into streamline density maps using the MRtrix3's tool 'tckmap' (Tournier et al. 2019). The streamline density maps were binarized, and a group-level overlap map was computed.

ROI-to-ROI structural and functional connectivity analysis

We used MRtrix3's tool 'tck2connectome' to analyze ROI-to-ROI structural connectivity. The cortical and subcortical ROIs were defined as stated in the previous section. Regarding ROI-to-ROI functional connectivity, we computed the partial correlation between the network nodes using the nilearn's function 'ConnectivityMeasure' (Pedregosa et al. 2011). The illustrations of the connectivity matrices were created with Matplotlib 3.4.2 (Hunter 2007).

Networks lateralization

We assessed the lateralization of the VAN and DAN networks. For functional connectivity, the average Pearson's correlation across each hemisphere's VAN and DAN nodes was calculated using the FSL's function 'fslmeants'. The obtained values were compared between the right and left hemispheres. For structural connectivity, we extracted the fiber tracts that crossed two nodes of the same hemisphere. Then, the fiber tracts were converted into volume maps using the MRtrix3's tool 'tckmap', and the individual volumes were compared between the two hemispheres (Tournier et al. 2019). Data were presented as mean (with standard deviations) or median (with interquartile ranges), and paired analyses were performed with paired t-test or Wilcoxon test, according to their distribution.

Graph theory analysis of structural connectivity

To analyze if the newly identified subcortical nuclei would be core regions in the networks, we performed a graph theory analysis of the hub properties of the VAN and DAN nodes. Two measures were used, the degree centrality and the betweenness centrality (Bullmore and Sporns 2009). Degree centrality denotes the fraction of nodes connected to the node of interest. Betweenness centrality is the fraction of all-

pairs shortest paths that pass through the node of interest (Bullmore and Sporns 2009). In graph theory, nodes with high centrality are considered network hubs, i.e., they play a crucial role in the global network function (van den Heuvel and Sporns 2013).

The 177 individual binarized structural connectivity matrices were converted into undirected connectivity graphs, and both measures were calculated using the NetworkX package (https://networkx.org/). ROIs, as defined in the previous sections, constituted the network nodes. The streamlines that crossed at least two ROIs defined network vertices. Considering the conservative parameters of our tractography adjusted over the years to match post-mortem Klingler dissections (Thiebaut de Schotten et al. 2011b; Catani et al. 2012; Vergani et al. 2014; Catani 2019), there was no threshold for the streamline considered for binarization. Additionally, streamline count does not accurately reflect the number of axonal projections between regions or the strength of connectivity (Gong et al. 2009; Jones et al. 2013), and previous work showed that the overall results of the network analysis do not change with modifications in the streamline count binarization threshold (Shu et al. 2011). Then, we calculated the median value of both measures across the 177 network graphs for each node. The illustrations of the network graphs were created with SurfIce (https://www.nitrc.org/projects/surfice/).

Structural correlations with the neurotransmitter system

We studied the relationship between the proposed neuroanatomical models' subcortical structural projections and the neurotransmitter systems' spatial distribution. First, we selected the newly identified brainstem nuclei that synthesize neurotransmitters, according to the cytochemical evidence in the literature. Second,

we computed the structural projections of these nuclei to the remaining nodes of the VAN and DAN, i.e., we selected the streamlines that crossed the brainstem nuclei of interest and every other node of the network, using the MRtrix3 tool 'tckedit' (Tournier et al. 2019). Then, we used the MRtrix3 tool 'tckmap' to map those streamlines into the MNI space (Tournier et al. 2019) and computed the individual Spearman's correlation between the spatial distribution of the created structural projection map and the neurotransmitter maps provided by Hansen and colleagues using the neuromaps' tool 'compare_images' (Hansen et al. 2021; Markello et al. 2022); https://netneurolab.github.io/neuromaps/). We obtained the correlation values distribution between the 110 individual VAN and DAN maps and each neurotransmitter map. To analyze if the obtained distributions (each composed by 110 correlation values) were significantly higher than zero, a non-parametric statistical test was performed (one-sided Wilcoxon test). The obtained p-values were corrected for multiple comparisons using the Bonferroni correction. Finally, we analyzed whether the correlation distributions were different between VAN and DAN, and if they were different between hemispheres (paired t-test or Wilcoxon test, according to data distribution; the Bonferroni correction was also applied). A supplemental pairwise analysis was performed. The average map of the 110 individual VAN and DAN structural projection maps was correlated with the neurotransmitter maps (Spearman's correlation; neuromaps' tool 'compare_images'; Markello et al. 2022; https://netneurolab.github.io/neuromaps/). To control for spatial autocorrelations and reduce the risk of false positive results, statistical significance was inferred based on null models generation (Alexander-Bloch et al. 2018; Burt et al. 2020; Markello and Misic 2021). Volumetric data was parcellated according to the Automated Anatomical Labeling atlas 3 (AAL3; Rolls et al. 2020), using the neuromaps' utility 'Parcellater'

(Markello et al. 2022; https://netneurolab.github.io/neuromaps/). AAL3 was chosen because it includes cortical and subcortical parcels. The null parcellations were generated from the average VAN and DAN structural projection maps using the neuromaps' function 'nulls.burt2020' (5000 permutations, generating 5000 null parcellations; Burt et al. 2020; Markello et al. 2022; https://netneurolab.github.io/neuromaps/). The graphical representations were created with Matplotlib 3.4.2 and Datashader 0.13.0 (Hunter 2007; https://datashader.org).

Results

VAN anatomical map

The statistical map of the VAN, after functional alignment, is represented in Figure 1 (left column).

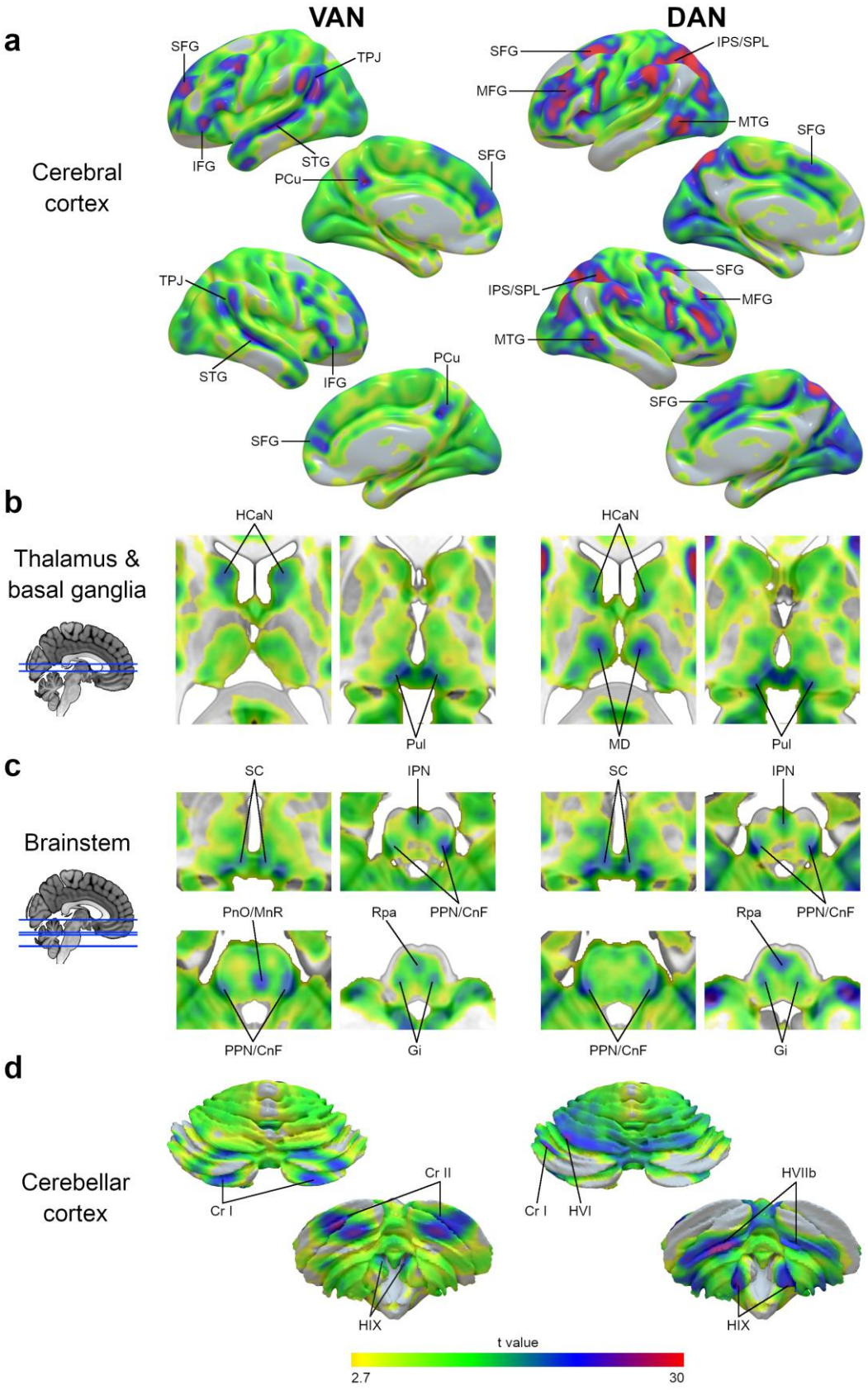

Figure 1. VAN (left) and DAN (right) maps after functional alignment at different anatomical levels, namely the cerebral cortical surface (a), subcortical thalamus and

basal ganglia (b), brainstem (c), and cerebellar cortical surface (d). The color gradient represents the t-value distribution. CnF, cuneiform nucleus; Cr I, cerebellar crus I lobule; Cr II, cerebellar crus II lobule; DAN, dorsal attention network; Gi, gigantocellular nucleus; HCaN, head of caudate nucleus; HIIb, cerebellar lobule IIb; HVI, cerebellar lobule VI; HIX, cerebellar lobule IX (cerebellar tonsils); IFG, inferior frontal gyrus; IPN, interpeduncular nucleus; IPS, intraparietal sulcus; MnR, median raphe nucleus; MD, mediodorsal nucleus of the thalamus; MTG, middle temporal gyrus; PCu, precuneus; PnO, nucleus pontis oralis; PPN, pedunculopontine nucleus; Pul, pulvinar; Rpa, raphe pallidus nucleus; SC, superior colliculus; SFG, superior frontal gyrus; SPL, superior parietal lobule; STG, superior temporal gyrus; TPJ, temporoparietal junction; VAN, ventral attention network.

At the cerebral cortical level, the peaks of statistical association were observed in the temporo-parietal junction, the inferior frontal gyrus, the anterior part of the superior frontal gyrus, and the superior temporal gyrus (Figure 1a). Additionally, peaks of statistical association were also present in the crus I, crus II and superior IX cerebellar cortex (Figure 1d).

A high statistical association was present at the thalamus and basal ganglia level in the head of caudate nuclei and the pulvinar (Figure 1b). In the brainstem, a high statistical association was observed in voxels overlapping with the superior colliculi, the interpeduncular nucleus, and the pedunculopontine-cuneiform nuclei complex pontis oralis, the gigantocellular nuclei, the raphe pallidus, and median nuclei (Figure 1c). Table 1 represents the centers of gravity coordinates of the subcortical regions of interest. The VAN statistical and correlation maps are available at https://neurovault.org/collections/XONZLGPJ/.

Table 1. MNI coordinates of the VAN subcortical regions' centers of gravity.

Regions of interest	MNI (X)	MNI (Y)	MNI (Z)
HCaN L	-11	8	13
Pul L	-4	-30	1
SC L	-9	-31	-3
PPN/CnF L	-14	-29	-25
Gi L	-10	-25	-36
Cr I L	-31	-73	-31
Cr II L	-21	-79	-42
IPN	1	-19	-21
MnR	-3	-29	-28
Rpa	1	-28	-43
HCaN R	13	11	12
Pul R	6	-29	1
SC R	13	-30	-3
PPN/CnF R	13	-31	-25
Gi R	11	-24	-35
Cr I R	30	-74	-30
Cr II R	24	-79	-41

CnF, cuneiform nucleus; Cr I, cerebellar crus I lobule; Cr II, cerebellar crus II lobule; Gi, gigantocellular nucleus; HCaN, head of caudate nucleus; IPN, interpeduncular nucleus; L, left; MnR, median raphe nucleus; PnO, nucleus pontis oralis; PPN, pedunculopontine nucleus; Pul, pulvinar; R, right; Rpa, raphe pallidus nucleus; SC, superior colliculus.

DAN anatomical map

The statistical map of the DAN, after functional alignment, is represented in Figure 1 (right column).

The peaks of the statistical association at the cerebral cortical level were in the intraparietal sulcus and superior parietal lobule, in the middle and superior frontal gyrus, and in the posterior part of the middle temporal gyrus (Figure 1a). Peaks of

statistical association were also present in the cerebellar cortex's areas VIIb, inferior IX, left VI, and left I (Figure 1d).

At the thalamus and basal ganglia level, areas with a high statistical association were located in the head of caudate nuclei and the thalamic pulvinar and mediodorsal nuclei (Figure 1b). High statistical associations also included voxels overlapping the superior colliculi, the interpeduncular nucleus, the pedunculopontine-cuneiform nuclei complex, the gigantocellular nuclei, and the raphe pallidus nuclei in the brain stem (Figure 1c). Table 2 represents the centers of gravity of the subcortical regions of interest. The DAN statistical and correlation maps are available at https://neurovault.org/collections/XONZLGPJ/.

Table 2. MNI coordinates of the DAN subcortical regions' centers of gravity.

Regions of interest	MNI (X)	MNI (Y)	MNI (Z)
HCaN L	-10	4	10
MD L	-9	-18	8
Pul L	-4	-30	1
SC L	-8	-31	-3
PPN/CnF L	-14	-30	-25
Gi L	-10	-24	-35
Cr I L	-39	-64	-29
HVI L	-25	-62	-24
HVIIb L	-24	-66	-49
HIX L	-11	-51	-50
IPN	1	-19	-21
Rpa	1	-28	-42
HCaN R	12	7	10
MD R	9	-16	8
Pul R	6	-29	1
SC R	11	-30	-3

PPN/CnF R	14	-30	-25
Gi R	11	-25	-34
HVIIb R	25	-68	-49
HIX R	11	-53	-51

CnF, cuneiform nucleus; Cr I, cerebellar crus I lobule; Gi, gigantocellular nucleus; HCaN, head of caudate nucleus; HVI, cerebellar lobule VI; HIX, cerebellar lobule IX (cerebellar tonsils); IPN, interpeduncular nucleus; L, left; MD, mediodorsal nucleus of the thalamus; PPN, pedunculopontine nucleus; Pul, pulvinar; R, right; Rpa, raphe pallidus nucleus; SC, superior colliculus.

The conjunction analysis showed that most of the subcortical peaks of statistical association were shared by both networks (Figure 2), explicitly overlapping the pulvinar, the superior colliculi, the interpeduncular nuclei, the pedunculopontine-cuneiform nuclei complex, the gigantocellular nuclei, and the raphe pallidus nuclei.

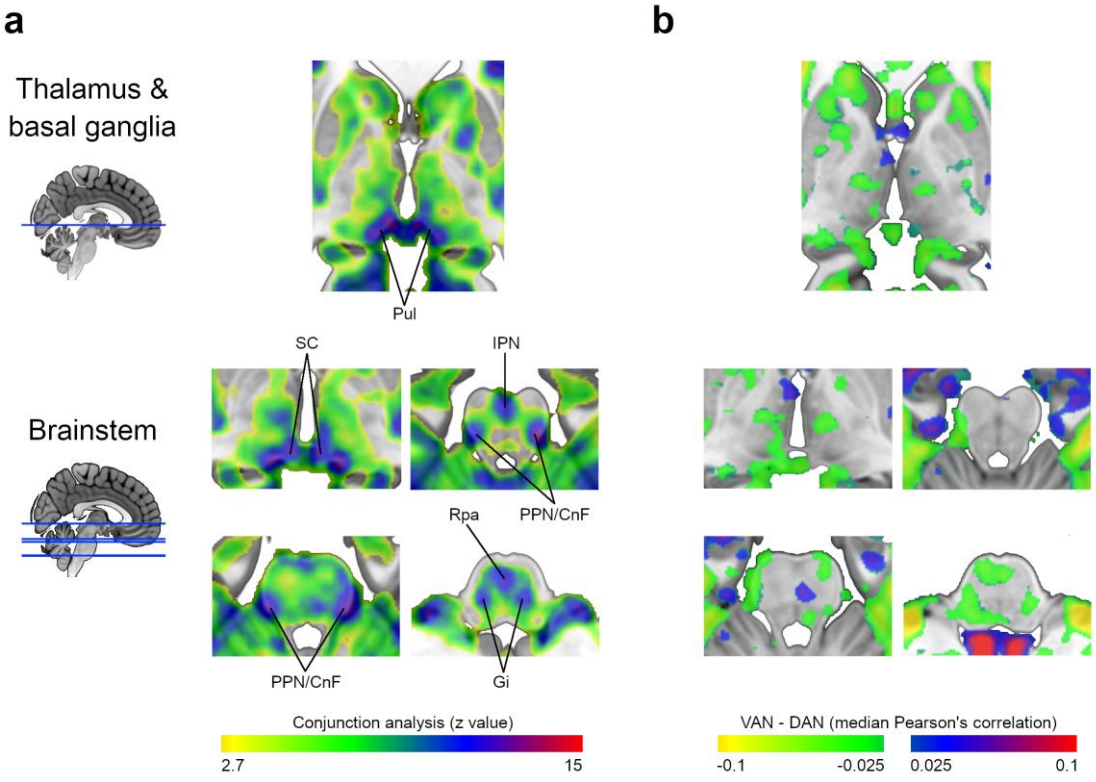

Figure 2. VAN and DAN maps similarity. (a) Conjunction analysis of the VAN and DAN statistical maps at the thalamus, basal ganglia, and brainstem levels. (b)

Difference map resulting from the subtraction of the median DAN Pearson's correlation map from the VAN. CnF, cuneiform nucleus; DAN, dorsal attention network; Gi, gigantocellular nucleus; IPN, interpeduncular nucleus; PPN, pedunculopontine nucleus; Pul, pulvinar; Rpa, raphe pallidus nucleus; SC, superior colliculus; VAN, ventral attention network. (see maps at https://neurovault.org/collections/XONZLGPJ/)

Structural and functional connectivity of the VAN nodes

The structural connectivity map of the VAN is represented in Figure 3a.

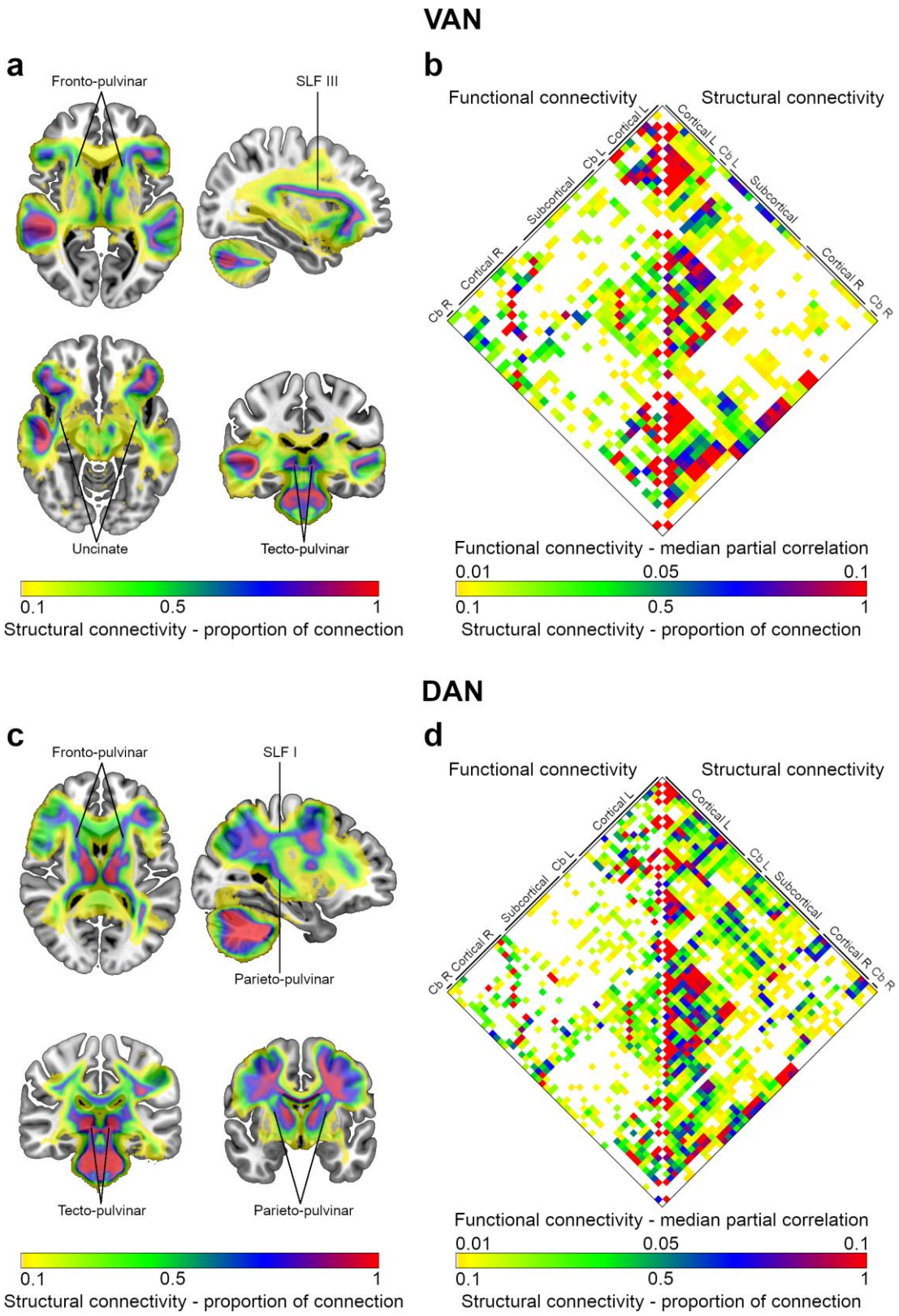

Figure 3. Structural and functional connectivity of VAN and DAN nodes. (a) Structural connectivity map of the VAN. (b) Matrix with the node-to-node functional

and structural connectivity of the VAN, represented on the left and right halves, respectively. (c) Structural connectivity map of the DAN. (d) Matrix with the node-to-node functional and structural connectivity of the DAN, represented on the left and right halves, respectively. Nodes of the matrices were labeled in groups according to their anatomical location. A complete list with node labels is available in Supplementary Tables 1 and 2. As indicated, color gradients represent the structural connectivity (expressed as the proportion of connection) or the functional connectivity (defined as the median partial correlation). Cb, cerebellum; L, left; R, right; SLF, superior longitudinal fasciculus.

The cortical regions of the VAN were connected by the third branch of the Superior Longitudinal Fasciculus (SLF III) and the uncinate fasciculus (Figure 3a). Fronto-pulvinar and tecto-pulvinar projections established the connections with or between subcortical structures (Figure 3a). The node-to-node structural and functional connectivity patterns are represented in Figure 3b.

The maps of the VAN ROIs and the structural connectivity analysis are available at https://neurovault.org/collections/XONZLGPJ/.

Structural and functional connectivity of DAN nodes

The structural connectivity map of the DAN is represented in Figure 3c.

The cortical regions of the DAN established connections through the first branch of the Superior Longitudinal Fasciculus (SLF I, Figure 3c). Fronto-pulvinar, parieto-pulvinar, and tecto-pulvinar projections mediated the links with or between subcortical structures (Figure 3c).

The node-to-node structural and functional connectivity patterns are shown in figure 3d.

The maps of the DAN ROIs and the structural connectivity analysis are available at https://neurovault.org/collections/XONZLGPJ/.

Lateralization assessment

Figure 4 illustrates the hemispheric distribution of the structural and functional connectivity measures of the VAN and the DAN.

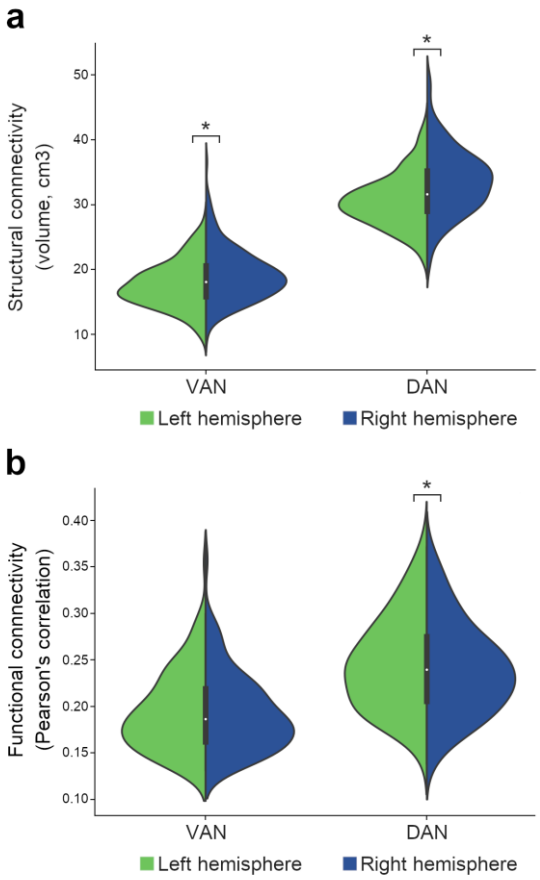

Figure 4. VAN and DAN lateralization. Structural connectivity is expressed in volumes of the structural connection maps (a) and functional connectivity in average Pearson's correlations (b) across hemispheric nodes. DAN, dorsal attention network;

VAN, ventral attention network. Asterisk (*), significant differences between the right and the left hemispheres (paired analysis).

The structural connectivity connecting the VAN was significantly larger in the right hemisphere than in the left (right hemisphere 18.7[16.5,21.1]cm^3, left hemisphere 17.0[15.3,19.7]cm^3; p-value<0.001). Pearson's correlations were not different between the right and left VANs (right hemisphere 0.185[0.162,0.218], left hemisphere 0.188[0.160,0.222]; p-value=0.125).

The DAN's structural connectivity was also significantly larger in the right hemisphere (right hemisphere 33.6[30.0,36.6]cm^3, left hemisphere 30.2[28.0,32.9]cm^3; p-value<0.001). Pearson's correlations were significantly higher in the left hemisphere than in the right (right hemisphere 0.240(0.049), left hemisphere 0.246(0.050); p-value<0.001).

Graph theory analysis

Figure 5a illustrates the graph theory representation of the VAN and DAN structural connectivity.

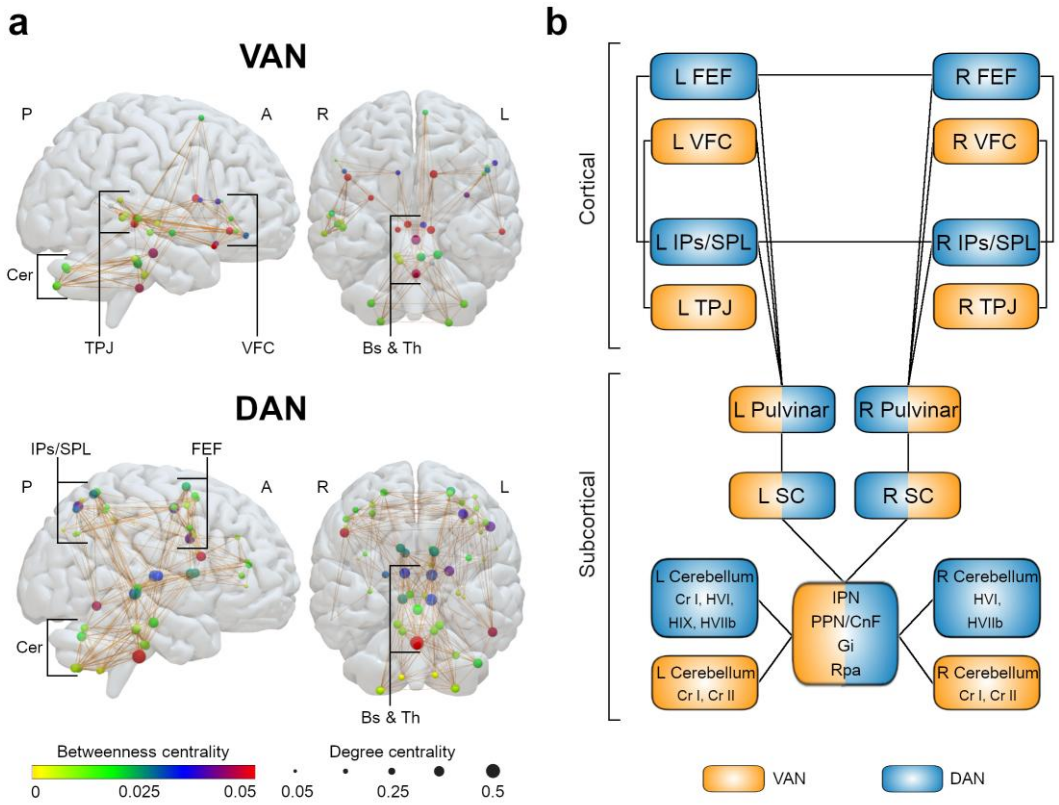

Figure 5. (a) Graph theory analysis of the DAN and VAN structural connectivity. Circles illustrate nodes. Circle colors represent the median betweenness centrality of each node (according to the color gradient), while circle dimensions represent the median degree centrality. Brown lines represent node-to-node structural connections present in at least half of the subjects. (b) Anatomical model of the VAN and DAN. A, anterior; CnF, cuneiform nucleus; DAN, dorsal attention network; Gi, gigantocellular nucleus; IPN, interpeduncular nucleus; L, left; P, posterior; PPN, pedunculopontine nucleus; Pul, pulvinar; R, right; Rpa, raphe pallidus nucleus; SC, superior colliculus; VAN, ventral attention network.

The subcortical structures with the highest median betweenness centrality in the VAN were in the right pulvinar and the left caudate nucleus head (the second and the third highest of all nodes, respectively). The highest median degree of centrality was

in the interpeduncular nucleus and the left pedunculopontine-cuneiform nuclei complex (the first and the second highest of all nodes, respectively).

In the DAN, the subcortical structures with the highest median betweenness centrality were the raphe pallidus nucleus and the right mediodorsal nucleus of the thalamus (the first and the seventh highest of all nodes, respectively). The highest median degree of centrality was the raphe pallidus nucleus and the left superior colliculus (the first and the second highest of all nodes, respectively).

Overall, the subcortical structures had high centrality values in both networks. The betweenness centrality and degree centrality values of all nodes in the VAN and the DAN are detailed in Supplementary Tables 3 and 4. The anatomical models of the VAN and DAN are illustrated in figure 5b.

Correlation with the neurotransmitter system

The brainstem nuclei identified in the VAN anatomical map that synthesize neurotransmitters are the pedunculopontine nuclei (cholinergic, glutamatergic, and GABAergic; Benarroch 2013), the cuneiform nuclei (glutamatergic and GABAergic; Chang et al. 2020), the gigantocellular nucleus (glutamatergic and GABAergic; Martin et al. 2011), the raphe nucleus (serotonergic; Van De Kar and Lorens 1979), and the raphe pallidus nucleus (serotonergic; Heym et al. 1982). The brainstem nuclei identified in the DAN anatomical map synthesizing neurotransmitters are the pedunculopontine, the cuneiform, the gigantocellular nuclei, and the raphe pallidus nucleus.

The spatial correlations of these brainstem nuclei structural projections with the neurotransmitter systems are represented in figure 6. The distributions of acetylcholine α4β2 nicotinic receptors, dopamine transporters, and serotonin

transporters were positively correlated with the distribution of VAN and DAN brainstem projections ($p<0.001$; figure 6a). The scatterplots representing the distributions of the significantly correlated systems are presented in figure 6b. Acetylcholine α4β2 nicotinic receptors and serotonin transporters had a higher spatial correlation with the VAN than with the DAN, whereas dopamine transporters had a higher spatial correlation with the DAN ($p<0.001$).

The supplemental pairwise correlation analyses between the average VAN and DAN structural projection maps and the neurotransmitter maps revealed similar results: the VAN had a significant positive spatial correlation with acetylcholine α4β2 nicotinic receptors and acetylcholine, dopamine, noradrenaline and serotonin transporters (Supplementary Table 5); the DAN had a significant positive spatial correlation with acetylcholine α4β2 nicotinic receptors and acetylcholine, dopamine and noradrenaline transporters (Supplementary Table 6).

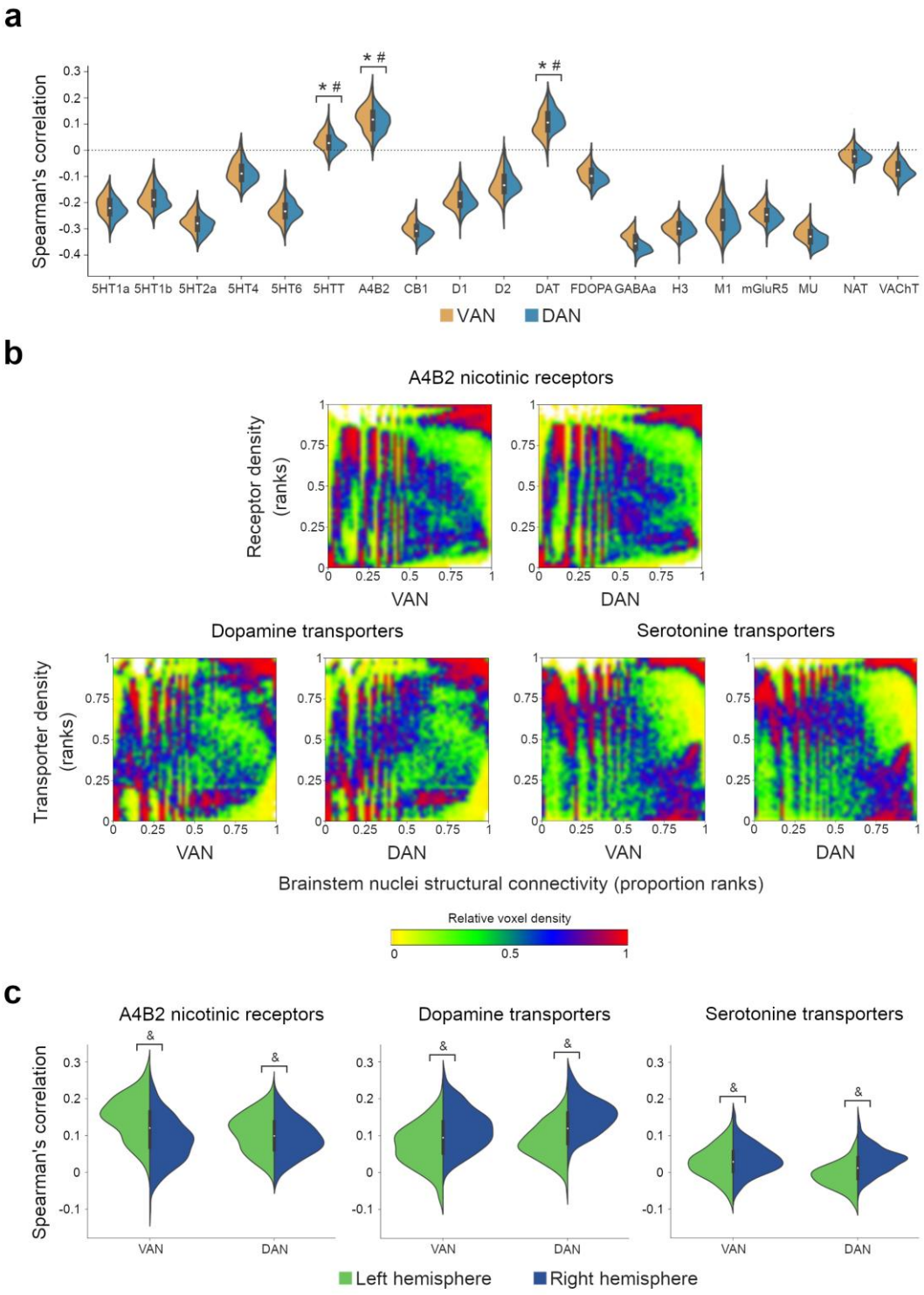

Figure 6. Correlation between the structural projections of the brainstem nuclei and the neurotransmitter systems. (a) Distributions of the Spearman's correlations for the available maps of neurotransmitter receptors and transporters; for the receptors or

transporters with two or more maps available, the mean correlation was calculated. (b) Graphical representation of the statistically significant positive correlations, i.e., the acetylcholine α4β2 nicotinic receptor, dopamine, and serotonin transporter maps. The color map represents the relative voxel density at each graph point. (c) Spearman's correlation of the statistically significant positive correlations with the left and right hemispheres. 5HT1a, serotonin 1a receptors; 5HT1b, serotonin 1b receptors; 5HT2a, serotonin 2a receptors; 5HTT, serotonin transporters; A4B2, acetylcholine α4β2 nicotinic receptors; CB1, cannabinoid receptors 1; D1, dopamine receptors 1; D2, dopamine receptors 2; DAT, dopamine transporters; FDOPA, fluorodopa; GABAa, GABAa receptors; H3, histamine receptors 3; M1, muscarinic receptors 1; mGluR5, metabotropic glutamate receptors 5; MU, mu-opioid receptors; NAT, noradrenaline transporters; VAchT, vesicular acetylcholine transporters. * Statistically significant positive correlation, corrected for multiple comparisons ($p<0.003$); # Statistically significant difference between the VAN and the DAN, corrected for multiple comparisons ($p<0.017$); & Statistically significant difference between right and left hemispheres, corrected for multiple comparisons ($p<0.017$).

The correlation of VAN and DAN brainstem projections with the acetylcholine α4β2 nicotinic receptors was significantly higher in the left hemisphere. In contrast, the correlations with the dopamine and serotonin transporters were higher in the right hemisphere (figure 6c).

Discussion

This study re-examined the VAN and the DAN neuroanatomy by co-registering individual network maps in a common functional space. We propose a new

comprehensive model of these networks based on the convergence of functional, structural, and neurochemical findings. First, we confirmed the initial hypothesis that subcortical structures, namely the pulvinar, the superior colliculi, the head of caudate nuclei, and a group of brainstem nuclei, are constituent elements of the attentional networks. Second, we characterized the structural connections underlying functional connectivity. Deep brain nuclei are densely connected and structural network hubs. Third, we showed that the identified brainstem nuclei projections are spatially correlated with the acetylcholine α4β2 nicotinic receptors and serotonin and dopamine transporters.

Pulvinar is a high-order thalamic relay nucleus participating in cortical-thalamocortical circuits that modulate information processing (Sherman 2007). Cytoarchitectonically, the pulvinar is divided into four regions: the anterior pulvinar, the inferior pulvinar, the medial pulvinar, and the lateral pulvinar (Stepniewska and Kaas 1997). The medial pulvinar is particularly important in establishing connections with heteromodal association areas, such as the superior and inferior temporal, the inferior parietal, the dorsolateral prefrontal, and the orbitofrontal cortices (Bridge et al. 2016). In our model, the pulvinar regions with the highest statistical level were medial, and we demonstrated that they were structurally connected with VAN cortical areas, through fronto-pulvinar projections, and with DAN cortical areas, by fronto-pulvinar and parieto-pulvinar projections (Bos and Benevento 1975; DeVito 1978; Lemaire et al. 2011). Pulvinar lesions may induce hemispatial neglect (Karnath et al. 2002). Decades ago, Sprague impressively found that hemispherectomy prompted symptoms of hemispatial neglect in cats which were attenuated by removing the contralesional superior colliculus (Sprague 1966; Krauzlis et al. 2013). This effect was later observed in humans (Weddell 2004). In our model, the pulvinar connects

with the superior colliculi through the tecto-pulvinar fibers (Luppino et al. 1988), demonstrating the importance of pulvinar - superior colliculi interactions in attention processes. Therefore, in the context of the so-called Sprague effect, removing the contralesional superior colliculus in cats with hemispatial neglect would damage the spared attentional network and might partially compensate for the imbalance in the attentional processing (Vuilleumier et al. 1996; Bartolomeo et al. 2007). Recently, hemispatial neglect was linked to lesions of the human superior colliculus (Nyffeler et al. 2021). The Sprague effect is also mediated by the pedunculopontine nuclei (Durmer and Rosenquist 2001; Valero-Cabré et al. 2020), which is one of the brainstem nuclei included in our model. The pedunculopontine nuclei possess a population of cholinergic neurons in their caudal portion, giving rise to a distinct network that regulates attentional states and enhances the processing of salient stimuli (Mena-Segovia and Bolam 2017). The descending projections from these cholinergic neurons innervate the nucleus pontis oralis (Mena-Segovia et al. 2008) and the gigantocellular nuclei (Martinez-Gonzalez et al. 2014), while their dorsal ascending projections innervate the colliculi (Jeon et al. 1993; Motts and Schofield 2009) and several nuclei of the thalamus, including the pulvinar and the mediodorsal nuclei (Steriade et al. 1988). The pattern of the pedunculopontine projections closely matches the brainstem and thalamic map evidenced in our analysis. Hence, lesion analyses and axonal tracings studies confirm the validity of our subcortical model of the VAN and the DAN.

The graph theory analysis results are consistent with the subcortical nuclei hub role in the VAN and the DAN organization. Centrality measures indicate how connected a node is with other nodes. These measures are considered surrogates of the node's relevance for the flow of information and communication within a network (Girvan

and Newman 2002; Bullmore and Sporns 2009). The DAN and the VAN subcortical nuclei had a high degree and betweenness centrality scores, positioning them as networks' core regions as previously suggested (Barabási and Albert 1999; Hagmann et al. 2008; Gong et al. 2009).

The neurotransmitter system correlation analysis reinforced the proposed relationship between the subcortical nuclei of the attention networks. The highest spatial correlation of both networks was with the acetylcholine α4β2 nicotinic receptors. The acetylcholine α4β2 nicotinic receptors have a well-established relationship with sustained attention. Acetylcholine α4β2 nicotinic receptors agonists reduce distractibility of adult monkeys during the performance of matching-to-sample tasks with distractors (Prendergast et al. 1998) and increase the firing rate of dorsolateral prefrontal neurons during sustained attention tasks, an effect that is reversed by the co-administration of receptor antagonists (Sun et al. 2017). In humans, transdermal nicotine administration improves attentiveness (Levin et al. 1998; Valentine and Sofuoglu 2017). All these observations in animals and humans support the critical role of the subcortical acetylcholinergic system in attentional processes.

The VAN and DAN brainstem nuclei projections were also spatially correlated with the distribution of dopamine and serotonin transporters. This finding is consistent with the psychopharmacological knowledge about attention. Methylphenidate is the first-line treatment for attention deficit hyperactivity disorder (Cortese et al. 2018). Pharmacologically, it is a noradrenaline-dopamine reuptake inhibitor with higher potency for dopamine transporters (Gatley et al. 1996; Faraone 2018). Modafinil is a selective inhibitor of dopamine transporters (Zolkowska et al. 2009) and produces attention enhancement effects (Turner et al. 2004; Repantis et al.

2010). Further studies are needed to understand how the interplay between the nicotinic acetylcholine and the dopamine systems occurs in attention networks, but it might be mediated by their interaction at the levels of the striatum (Zoli et al. 2002; Exley and Cragg 2008) and midbrain (Blaha and Winn 1993; Forster and Blaha 2003). Serotonin reuptake inhibitors also modulate attentional processes (Harmer and Cowen 2013). They increase the perceptual bias towards emotional stimuli (Harmer et al. 2004; Browning et al. 2007) by regulating the activity of visual processing circuits (Harmer and Cowen 2013). Therefore, our improved model of the DAN and VAN functional neuroanatomy appears to reconcile previous neuroimaging and pharmacological findings. As previously suggested (Corbetta et al. 2008), additional pharmacological studies will be required to understand the preferential association of VAN with acetylcholine α4β2 nicotinic receptors. Similarly pharmacological studies are required to shed light on the effect of serotonin transporter on the VAN and to reveal the relationship between dopamine transporters and the DAN. Finally, understanding the relationship between the neurochemical signature and hemispheric functional dominance still require more research in animals and humans (Corbetta et al. 2008).

Characterizing the human brain's subcortical anatomy of attention networks fosters the exploration of a common structural-functional attentional framework across species. Attention is far from being a specific cognitive ability of human beings (Washburn and Taglialatela 2006). Species with either close or distant common ancestors in the phylogenetic tree, such as monkeys, rats, and pigeons, can scan, select and maintain attention to surrounding environmental stimuli (Mackintosh 1965; Blough 1977; Washburn and Taglialatela 2006; Wasserman and Castro 2021). A common subcortical attention framework may surpass the challenge of finding the

cortical homologs of the human VAN and DAN in other species (Patel et al. 2015). Accordingly, future studies might use the subcortical areas we highlighted to explore comparatively the organization of the VAN and the DAN in non-human species.

In our analysis, VAN and DAN structural connectivity maps were right-lateralized. The right lateralization of the VAN is established in the literature. Evidence demonstrates that the SLF III has a larger volume in the right hemisphere and that its anatomical lateralization correlates with visuomotor processing abilities and the asymmetries of visuospatial task performance (Thiebaut de Schotten et al. 2011a; Chechlacz et al. 2015; Budisavljevic et al. 2017; Cazzoli and Chechlacz 2017; Howells et al. 2018; Amemiya et al. 2021). The SLF I, the main tract connecting DAN cortical regions, does not show a preferential lateralization (Thiebaut de Schotten et al. 2011a; Amemiya et al. 2021). However, some DAN areas might be right-lateralized (Bartolomeo and Seidel Malkinson 2019). The right intraparietal sulcus (Sheremata and Silver 2015) and frontal eye field (Szczepanski et al. 2010) increase their activity for both visual fields, while the left preferentially reacts to contralateral stimulations. The processing of both visual fields in the right hemisphere is corroborated by right hemisphere stroke patients with hemispatial neglect who also present with deficits in goal-driven selective attention for ipsilateral stimuli (Snow and Mattingley 2006). Hence, while the cortical extent of the DAN was not asymmetrical, our structural connectivity analysis, including the cortico-subcortical projection tracts, might have the function-specific dimension of the right-lateralization of the DAN.

Regarding functional connectivity, the distribution of VAN was not different between hemispheres, and the DAN was slightly left-lateralized. Task-based *f*MRI studies indicate right lateralization of the VAN (Downar et al. 2000; Fox et al. 2006),

but the asymmetry might vary according to the nature of the task (Doricchi et al. 2010). Accordingly, while functional asymmetry is expected for some task-related activations (Shulman et al. 2010), resting-state functional connectivity may not capture function-specific asymmetries due to its global nature.

A limitation of our study is the inability to untangle the different roles and dynamic interactions between the proposed subcortical structures. While the cortical regions of the DAN and the VAN are quite neatly segregated (Vossel et al. 2014), the subcortical nuclei described in our model probably contributed to both the VAN and the DAN. Future investigations using our model to explore the BOLD signal during task-related *f*MRI in humans or direct electrical recordings in animals might better dissociate the hierarchical organization and functional role of subcortical regions than resting-state *f*MRI. In addition, the neurotransmitter systems normative atlas is derived from different samples (Hansen et al. 2021). As PET and SPECT tracers are radioactive, it is not possible to map several neurotransmitter systems in the same participants. Although the atlas was replicated in an independent autoradiography dataset and all scans were acquired in healthy volunteers (Hansen et al. 2021), the heterogeneity of the data sources may represent a limitation for its interpretation.

In conclusion, this work proposes an improved neuroanatomical model of the VAN and the DAN that includes the pulvinar, the superior colliculi, the head of caudate nuclei, and a group of brainstem nuclei interrelated with the acetylcholine nicotinic and the dopamine and serotonin transporter systems. This novel framework reconciles behavioral, electrophysiological, and psychopharmacological data and provides a shared foundation to explore the neural basis of attention across different species and brain pathologies.

Acknowledgments

This project has received funding from the European Research Council (ERC) under the European Union's Horizon 2020 research and innovation programme (grant agreement No. 818521; MTS), the Marie Skłodowska-Curie programme (grant agreement No. 101028551; SJF), a Donders Mohrmann Fellowship (SJF, No. 2401512), "Prémio João Lobo Antunes 2018" – SCML (PNA), and "Bolsa de Investigação em Doenças Vasculares Cerebrais 2017" – SPAVC (PNA).

MC was supported by MIUR - Departments of Excellence Italian Ministry of Research (MART_ECCELLENZA18_01); Fondazione Cassa di Risparmio di Padova e Rovigo (CARIPARO)(Grant Agreement number 55403); Ministry of Health Italy NEUROCONN (RF-2008 -12366899); Celeghin Foundation Padova (CUP C94I20000420007); BIAL foundation grant (No. 361/18); H2020 European School of Network Neuroscience- euSNN, H2020-SC5-2019-2, (Grant Agreement number 869505); H2020 VARCITIES, H2020-SC5-2019-2 (Grant Agreement number 869505); Ministry of Health Italy: EYEMOVINSTROKE (RF-2019-12369300).

Data were provided by the McDonnell Center for Systems Neuroscience at Washington University.

Data availability statement

The presented brain maps are openly available at https://neurovault.org/collections/XONZLGPJ/, the resting-state functional 7T MRI datasets in the Human Connectome Project S1200 dataset, and the processed tractographies at http://opendata.bcblab.com.

Code availability statement

Analyses were conducted using open software and toolboxes, as specified in the methods. The Funcon-Connectivity code is openly available at https://github.com/chrisfoulon/BCBToolKit; the ANTs scripts 'buildtemplateparallel.sh' and 'WarpImageMultiTransform' at https://github.com/ANTsX/ANTs; the code where these scripts were applied for the functional alignment performed in this work at https://github.com/Pedro-N-Alves/VAN_DAN_functional_alignment; the 'easythresh_conj.sh' code (used for the conjunction analysis) at https://warwick.ac.uk/fac/sci/statistics/staff/academic-research/nichols/; the 'tckedit', 'tckmap' and 'tck2connectome' commands' codes at https://github.com/MRtrix3/mrtrix3; the 'ConnectivityMeasure' script at https://github.com/nilearn/nilearn/; the 'betweenness_centrality' and 'degree_centrality' scripts at https://github.com/networkx/networkx; and the 'compare_images', 'Parcellater' and 'nulls.burt202' scripts at https://github.com/netneurolab/neuromaps.

References

Alexander-Bloch AF, Shou H, Liu S, et al (2018) On testing for spatial correspondence between maps of human brain structure and function. Neuroimage 178:540–551. https://doi.org/10.1016/j.neuroimage.2018.05.070

Alves PN, Foulon C, Karolis V, et al (2019) An improved neuroanatomical model of the default-mode network reconciles previous neuroimaging and neuropathological findings. Commun Biol 2:370. https://doi.org/10.1038/s42003-019-0611-3

Amemiya K, Naito E, Takemura H (2021) Age dependency and lateralization in the three branches of the human superior longitudinal fasciculus. Cortex 139:116–133. https://doi.org/10.1016/j.cortex.2021.02.027

Amunts K, Kedo O, Kindler M, et al (2005) Cytoarchitectonic mapping of the human amygdala, hippocampal region and entorhinal cortex: Intersubject variability and probability maps. Anat Embryol (Berl) 210:343–352. https://doi.org/10.1007/s00429-005-0025-5

Amunts K, Lepage C, Borgeat L, et al (2013) BigBrain: An ultrahigh-resolution 3D human brain model. Science (80-) 340:1472–1475. https://doi.org/10.1126/science.1235381

Aston-Jones G, Rajkowski J, Cohen J (1999) Role of locus coeruleus in attention and behavioral flexibility. Biol Psychiatry 46:1309–1320. https://doi.org/10.1016/S0006-3223(99)00140-7

Avants BB, Epstein CL, Grossman M, Gee JC (2008) Symmetric diffeomorphic image registration with cross-correlation: Evaluating automated labeling of elderly and neurodegenerative brain. Med Image Anal 12:26–41. https://doi.org/10.1016/j.media.2007.06.004

Avants BB, Tustison NJ, Song G, et al (2011) A reproducible evaluation of ANTs similarity metric performance in brain image registration. Neuroimage 54:2033–2044. https://doi.org/10.1016/j.neuroimage.2010.09.025

Baldassarre A, Ramsey L, Hacker CL, et al (2014) Large-scale changes in network interactions as a physiological signature of spatial neglect. Brain 137:3267–3283. https://doi.org/10.1093/brain/awu297

Barabási A-L, Albert R (1999) Emergence of Scaling in Random Networks Downloaded from. Science (80-) 286:509–12. https://doi.org/10.1126/science.286.5439.509

Bartolomeo P (2013) Attention Disorders After Right Brain Damage: Living in Halved Worlds, 2014th edn. Springer

Bartolomeo P, Seidel Malkinson T (2019) Hemispheric lateralization of attention processes in the human brain. Curr Opin Psychol 29:90–96. https://doi.org/10.1016/j.copsyc.2018.12.023

Bartolomeo P, Thiebaut De Schotten M, Doricchi F (2007) Left unilateral neglect as a disconnection syndrome. Cereb Cortex 17:2479–2490. https://doi.org/10.1093/cercor/bhl181

Behrens TEJ, Johansen-Berg H, Woolrich MW, et al (2003) Non-invasive mapping of connections between human thalamus and cortex using diffusion imaging. Nat Neurosci 6:750–757. https://doi.org/10.1038/nn1075

Benarroch EE (2013) Pedunculopontine nucleus: Functional organization and clinical implications. Neurology 80:1148–1155. https://doi.org/10.1212/WNL.0b013e3182886a76

Bender DB, Youakim M (2001) Effect of attentive fixation in macaque thalamus and cortex. J Neurophysiol 85:219–234. https://doi.org/10.1152/jn.2001.85.1.219
Blaha CD, Winn P (1993) Modulation of dopamine efflux in the striatum following cholinergic stimulation of the substantia nigra in intact and pedunculopontine tegmental nucleus-lesioned rats. J Neurosci 13:1035–1044. https://doi.org/10.1523/jneurosci.13-03-01035.1993
Blough DS (1977) Visual search in the pigeon: Hunt and peck method. Science (80-) 196:1013–4. https://doi.org/10.1126/science.860129
Bos J, Benevento LA (1975) Projections of the medial pulvinar to orbital cortex and frontal eye fields in the rhesus monkey (Macaca mulatta). Exp Neurol 49:487–496. https://doi.org/10.1016/0014-4886(75)90103-X
Bouret S, Sara SJ (2005) Network reset: A simplified overarching theory of locus coeruleus noradrenaline function. Trends Neurosci 28:574–582. https://doi.org/10.1016/j.tins.2005.09.002
Brett M, Johnsrude IS, Owen AM (2002) The problem of functional localization in the human brain. Nat Rev Neurosci 3:243–249
Bridge H, Leopold DA, Bourne JA (2016) Adaptive Pulvinar Circuitry Supports Visual Cognition. Trends Cogn Sci 20:146–157. https://doi.org/10.1016/j.tics.2015.10.003
Browning M, Reid C, Cowen PJ, et al (2007) A single dose of citalopram increases fear recognition in healthy subjects. J Psychopharmacol 21:684–690. https://doi.org/10.1177/0269881106074062
Budisavljevic S, Dell'Acqua F, Zanatto D, et al (2017) Asymmetry and Structure of the Fronto-Parietal Networks Underlie Visuomotor Processing in Humans. Cereb Cortex 27:1532–1544. https://doi.org/10.1093/cercor/bhv348
Bullmore E, Sporns O (2009) Complex brain networks: Graph theoretical analysis of structural and functional systems. Nat Rev Neurosci 10:186–198. https://doi.org/10.1038/nrn2575
Burt JB, Helmer M, Shinn M, et al (2020) Generative modeling of brain maps with spatial autocorrelation. Neuroimage 220:117038. https://doi.org/10.1016/j.neuroimage.2020.117038
Buschman TJ, Miller EK (2007) Top-down versus bottom-up control of attention in the prefrontal and posterior parietal cortices. Science (80-) 315:1860–1864. https://doi.org/10.1126/science.1138071
Carmack PS, Spence J, Gunst RF, et al (2004) Improved agreement between Talairach and MNI coordinate spaces in deep brain regions. Neuroimage 22:367–371. https://doi.org/10.1016/j.neuroimage.2004.01.022
Catani M (2019) The anatomy of the human frontal lobe, 1st edn. Elsevier B.V.
Catani M, Dell'Acqua F, Vergani F, et al (2012) Short frontal lobe connections of the human brain. Cortex 48:273–291. https://doi.org/10.1016/j.cortex.2011.12.001
Catani M, Thiebaut de Schotten M (2012) Atlas of Human Brain Connections, 1st editio. Oxford University Press
Cazzoli D, Chechlacz M (2017) A matter of hand: Causal links between hand dominance, structural organization of fronto-parietal attention networks, and variability in behavioural responses to transcranial magnetic stimulation. Cortex 86:230–246. https://doi.org/10.1016/j.cortex.2016.06.015
Chakravarty MM, Bertrand G, Hodge CP, et al (2006) The creation of a brain atlas for image guided neurosurgery using serial histological data. Neuroimage 30:359–376. https://doi.org/10.1016/j.neuroimage.2005.09.041
Chang SJ, Cajigas I, Opris I, et al (2020) Dissecting Brainstem Locomotor Circuits:

Converging Evidence for Cuneiform Nucleus Stimulation. Front Syst Neurosci 14:1–8. https://doi.org/10.3389/fnsys.2020.00064
Chechlacz M, Gillebert CR, Vangkilde SA, et al (2015) Structural variability within frontoparietal networks and individual differences in attentional functions: An approach using the theory of visual attention. J Neurosci 35:10647–10658. https://doi.org/10.1523/JNEUROSCI.0210-15.2015
Cohen J (1988) Statistical power analysis for the behavioural sciences, 2nd edn. Lawrence Erlbaum Associates
Conroy BR, Singer BD, Guntupalli JS, et al (2013) Inter-subject alignment of human cortical anatomy using functional connectivity. Neuroimage 81:400–411. https://doi.org/10.1016/j.neuroimage.2013.05.009
Corbetta M, Kincade JM, Ollinger JM, et al (2000) Voluntary orienting is dissociated from target detection in human posterior parietal cortex. Nat Neurosci 3:. https://doi.org/10.1038/73009
Corbetta M, Kincade MJ, Lewis C, et al (2005) Neural basis and recovery of spatial attention deficits in spatial neglect. Nat Neurosci 8:1603–1610. https://doi.org/10.1038/nn1574
Corbetta M, Patel G, Shulman GL (2008) The Reorienting System of the Human Brain: From Environment to Theory of Mind. Neuron 58:306–324. https://doi.org/10.1016/j.neuron.2008.04.017
Corbetta M, Shulman GL (2002) Control of goal-directed and stimulus-driven attention in the brain. Nat Rev Neurosci 3:201–15. https://doi.org/10.1038/nrn755
Corbetta M, Shulman GL (2011) Spatial neglect and attention networks
Cortese S, Adamo N, Del Giovane C, et al (2018) Comparative efficacy and tolerability of medications for attention-deficit hyperactivity disorder in children, adolescents, and adults: a systematic review and network meta-analysis. The Lancet Psychiatry 5:727–738. https://doi.org/10.1016/S2215-0366(18)30269-4
Dell'Acqua F, Scifo P, Rizzo G, et al (2010) A modified damped Richardson-Lucy algorithm to reduce isotropic background effects in spherical deconvolution. Neuroimage 49:1446–1458. https://doi.org/10.1016/j.neuroimage.2009.09.033
DeVito JL (1978) A horseradish peroxidase-autoradiographic study of parietopulvinar connections in saimiri sciureus. Exp Brain Res 32:581–590. https://doi.org/10.1007/BF00239554
Doricchi F, MacCi E, Silvetti M, MacAluso E (2010) Neural correlates of the spatial and expectancy components of endogenous and stimulus-driven orienting of attention in the posner task. Cereb Cortex 20:1574–1585. https://doi.org/10.1093/cercor/bhp215
Downar J, Crawley AP, Mikulis DJ, Davis KD (2000) A multimodal cortical network for the detection of changes in the sensory environment. Nat Neurosci 3:277–283. https://doi.org/10.1038/72991
Durmer JS, Rosenquist AC (2001) Ibotenic acid lesions in the pedunculopontine region result in recovery of visual orienting in the hemianopic cat. Neuroscience 106:765–781. https://doi.org/10.1016/S0306-4522(01)00321-9
Eickhoff SB, Yeo BTT, Genon S (2018) Imaging-based parcellations of the human brain. Nat Rev Neurosci 19:672–686. https://doi.org/10.1038/s41583-018-0071-7
Ewert S, Plettig P, Li N, et al (2018) Toward defining deep brain stimulation targets in MNI space: A subcortical atlas based on multimodal MRI, histology and structural connectivity. Neuroimage 170:271–282. https://doi.org/10.1016/j.neuroimage.2017.05.015

Exley R, Cragg SJ (2008) Presynaptic nicotinic receptors: A dynamic and diverse cholinergic filter of striatal dopamine neurotransmission. Br J Pharmacol 153:283–297. https://doi.org/10.1038/sj.bjp.0707510
Faraone S V. (2018) The pharmacology of amphetamine and methylphenidate: Relevance to the neurobiology of attention-deficit/hyperactivity disorder and other psychiatric comorbidities. Neurosci Biobehav Rev 87:255–270. https://doi.org/10.1016/j.neubiorev.2018.02.001
Ferro JM, Martins IP, Távora L (1984) Neglect in children. Ann Neurol 15:281–284. https://doi.org/10.1002/ana.410150314
Fischl B, Rajendran N, Busa E, et al (2008) Cortical folding patterns and predicting cytoarchitecture. Cereb Cortex 18:1973–1980. https://doi.org/10.1093/cercor/bhm225
Foote SL, Morrison JH (1987) Extrathalamic modulation of cortical function. Annu Rev Neurosci 10:67–95. https://doi.org/10.1146/annurev.ne.10.030187.000435
Forster GL, Blaha CD (2003) Pedunculopontine tegmental stimulation evokes striatal dopamine efflux by activation of acetylcholine and glutamate receptors in the midbrain and pons of the rat. Eur J Neurosci 17:751–762. https://doi.org/10.1046/j.1460-9568.2003.02511.x
Foulon C, Cerliani L, Kinkingnéhun S, et al (2018) Advanced lesion symptom mapping analyses and implementation as BCBtoolkit. Gigascience 7:1–17. https://doi.org/10.1093/gigascience/giy004
Fox MD, Corbetta M, Snyder AZ, et al (2006) Spontaneous neuronal activity distinguishes human dorsal and ventral attention systems. Proc Natl Acad Sci U S A 103:10046–10051. https://doi.org/10.1073/pnas.0604187103
Gatley SJ, Pan D, Chen R, et al (1996) Affinities of methylphenidate derivatives for dopamine, norepinephrine and serotonin transporters. Life Sci 58:231–239. https://doi.org/10.1016/0024-3205(96)00052-5
Girvan M, Newman MEJ (2002) Community structure in social and biological networks. Proc Natl Acad Sci U S A 99:7821–7826. https://doi.org/10.1073/pnas.122653799
Glasser MF, Coalson TS, Robinson EC, et al (2016) A multi-modal parcellation of human cerebral cortex. Nature 536:171–178. https://doi.org/10.1038/nature18933
Glasser MF, Sotiropoulos SN, Wilson JA, et al (2013) The minimal preprocessing pipelines for the Human Connectome Project. Neuroimage 80:105–124. https://doi.org/10.1016/j.neuroimage.2013.04.127
Gong G, He Y, Concha L, et al (2009) Mapping Anatomical Connectivity Patterns of Human Cerebral Cortex Using In Vivo Diffusion Tensor Imaging Tractography. Cereb Cortex 19:524–536. https://doi.org/10.1093/cercor/bhn102
Gordon EM, Laumann TO, Adeyemo B, et al (2016) Generation and Evaluation of a Cortical Area Parcellation from Resting-State Correlations. Cereb Cortex 26:288–303. https://doi.org/10.1093/cercor/bhu239
Guntupalli JS, Hanke M, Halchenko YO, et al (2016) A Model of Representational Spaces in Human Cortex. Cereb Cortex 26:2919–2934. https://doi.org/10.1093/cercor/bhw068
Hagmann P, Cammoun L, Gigandet X, et al (2008) Mapping the structural core of human cerebral cortex. PLoS Biol 6:1479–1493. https://doi.org/10.1371/journal.pbio.0060159
Hansen JY, Shafiei G, Markello RD, et al (2021) Mapping neurotransmitter systems to the structural and functional organization of the human neocortex. bioRxiv

2021.10.28.466336. https://doi.org/10.1101/2021.10.28.466336
Harmer CJ, Cowen PJ (2013) 'It's the way that you look at it'-a cognitive neuropsychological account of SSRI action in depression. Philos Trans R Soc B Biol Sci 368:. https://doi.org/10.1098/rstb.2012.0407
Harmer CJ, Shelley NC, Cowen PJ, Goodwin GM (2004) Increased positive versus negative affective perception and memory in healthy volunteers following selective serotonin and norepinephrine reuptake inhibition. Am J Psychiatry 161:1256–1263. https://doi.org/10.1176/appi.ajp.161.7.1256
Haxby J V., Guntupalli JS, Connolly AC, et al (2011) A common, high-dimensional model of the representational space in human ventral temporal cortex. Neuron 72:404–416. https://doi.org/10.1016/j.neuron.2011.08.026
Haxby J V., Guntupalli JS, Nastase SA, Feilong M (2020) Hyperalignment: Modeling shared information encoded in idiosyncratic cortical topographies. Elife 9:1–26. https://doi.org/10.7554/eLife.56601
He BJ, Snyder AZ, Vincent JL, et al (2007) Breakdown of Functional Connectivity in Frontoparietal Networks Underlies Behavioral Deficits in Spatial Neglect. Neuron 53:905–918. https://doi.org/10.1016/j.neuron.2007.02.013
Healton EB, Navarro C, Bressman S, Brust JCM (1982) Subcortical neglect. Neurology 32:776–778. https://doi.org/10.1212/wnl.32.7.776
Heym J, Steinfels GF, Jacobs BL (1982) Activity of serotonin-containing neurons in the nucleus raphe pallidus of freely moving cats. Brain Res 251:259–276. https://doi.org/10.1016/0006-8993(82)90743-0
Howells H, De Schotten MT, Dell'Acqua F, et al (2018) Frontoparietal tracts linked to lateralized hand preference and manual specialization. Cereb Cortex 28:1–13. https://doi.org/10.1093/cercor/bhy040
Hunter J (2007) Matplotlib: a 2D graphics environment. Comput Sci Eng 9:90–95. https://doi.org/10.1109/MCSE.2007.55
Ivanov I, Bansal R, Hao X, et al (2010) Morphological Abnormalities of the Thalamus in Youths With Attention Deficit Hyperactivity Disorder. Image Process 397–408. https://doi.org/10.1176/appi.ajp.2009.09030398
James W (1890) The principles of psychology. Henry Holt and Company, New York
Jenkinson M, Bannister P, Brady M, Smith S (2002) Improved optimization for the robust and accurate linear registration and motion correction of brain images. Neuroimage 17:825–841. https://doi.org/10.1016/S1053-8119(02)91132-8
Jenkinson M, Beckmann CF, Behrens TEJ, et al (2012) Fsl. Neuroimage 62:782–790. https://doi.org/10.1016/j.neuroimage.2011.09.015
Jeon C -J, Spencer RF, Mize RR (1993) Organization and synaptic connections of cholinergic fibers in the cat superior colliculus. J Comp Neurol 333:360–374. https://doi.org/10.1002/cne.903330305
Jones DK, Knösche TR, Turner R (2013) White matter integrity, fiber count, and other fallacies: The do's and don'ts of diffusion MRI. Neuroimage 73:239–254. https://doi.org/10.1016/j.neuroimage.2012.06.081
Karnath HO, Himmelbach M, Rorden C (2002) The subcortical anatomy of human spatial neglect: Putamen, caudate nucleus and pulvinar. Brain 125:350–360. https://doi.org/10.1093/brain/awf032
Kenney J (1939) Mathematics of Statistics. Chapman & Hall, London
Klein A, Andersson J, Ardekani BA, et al (2009) Evaluation of 14 nonlinear deformation algorithms applied to human brain MRI registration. Neuroimage 46:786–802. https://doi.org/10.1016/j.neuroimage.2008.12.037
Krauzlis RJ, Lovejoy LP, Zénon A (2013) Superior Colliculus and Visual Spatial

Attention. Annu Rev Neurosci 36:. https://doi.org/10.1146/annurev-neuro-062012-170249.Superior
Langs G, Golland P, Ghosh S (2015) Predicting Activation Across Individuals with Resting-State Functional Connectivity Based Multi-Atlas Label Fusion. Med Image Comput Comput Assist Interv 9350:313–320. https://doi.org/10.1007/978-3-319-24571-3
Lechanoine F, Jacquesson T, Beaujoin J, et al (2021) WIKIBrainStem: An online atlas to manually segment the human brainstem at the mesoscopic scale from ultrahigh field MRI. Neuroimage 236:. https://doi.org/10.1016/j.neuroimage.2021.118080
Lemaire JJ, Cosnard G, Sakka L, et al (2011) White matter anatomy of the human deep brain revisited with high resolution DTI fibre tracking. Neurochirurgie 57:52–67. https://doi.org/10.1016/j.neuchi.2011.04.001
Levin ED, Conners CK, Silva D, et al (1998) Transdermal nicotine effects on attention. Psychopharmacology (Berl) 140:135–141. https://doi.org/10.1007/s002130050750
Li R, Wu X, Fleisher AS, et al (2012) Attention-related networks in Alzheimer's disease: A resting functional MRI study. Hum Brain Mapp 33:1076–1088. https://doi.org/10.1002/hbm.21269
Luo L, Rodriguez E, Jerbi K, et al (2010) Ten years of Nature Reviews Neuroscience: Insights from the highly cited. Nat Rev Neurosci 11:718–726. https://doi.org/10.1038/nrn2912
Luppino G, Matelli M, Carey RG, et al (1988) New view of the organization of the pulvinar nucleus in Tupaia as revealed by tectopulvinar and pulvinar-cortical projections. J Comp Neurol 273:67–86. https://doi.org/10.1002/cne.902730107
Mackintosh NJ (1965) Selective attention in animal discrimination learning. Psychol Bull 64:124–150. https://doi.org/10.1037/h0022347
Markello RD, Hansen JY, Liu Z-Q, et al (2022) Neuromaps: structural and functional interpretation of brain maps. bioRxiv 2022.01.06.475081
Markello RD, Misic B (2021) Comparing spatial null models for brain maps. Neuroimage 236:118052. https://doi.org/10.1016/j.neuroimage.2021.118052
Martin EM, Devidze N, Shelley DN, et al (2011) Molecular and neuroanatomical characterization of single neurons in the mouse medullary gigantocellular reticular nucleus. J Comp Neurol 519:2574–2593. https://doi.org/10.1002/cne.22639
Martinez-Gonzalez C, Van Andel J, Bolam JP, Mena-Segovia J (2014) Divergent motor projections from the pedunculopontine nucleus are differentially regulated in Parkinsonism. Brain Struct Funct 219:1451–1462. https://doi.org/10.1007/s00429-013-0579-6
McCarthy H, Skokauskas N, Mulligan A, et al (2013) Attention network hypoconnectivity with default and affective network hyperconnectivity in adults diagnosed with attention-deficit/hyperactivity disorder in childhood. JAMA Psychiatry 70:1329–1337. https://doi.org/10.1001/jamapsychiatry.2013.2174
Mena-Segovia J, Bolam JP (2017) Rethinking the Pedunculopontine Nucleus: From Cellular Organization to Function. Neuron 94:7–18. https://doi.org/10.1016/j.neuron.2017.02.027
Mena-Segovia J, Sims HM, Magill PJ, Bolam JP (2008) Cholinergic brainstem neurons modulate cortical gamma activity during slow oscillations. J Physiol 586:2947–2960. https://doi.org/10.1113/jphysiol.2008.153874
Morrison JH, Foote SL (1986) Noradrenergic and serotoninergic innervation of

cortical, thalamic, and tectal visual structures in old and new world monkeys. J Comp Neurol 243:117–138. https://doi.org/10.1002/cne.902430110
Motts SD, Schofield BR (2009) Sources of cholinergic input to the inferior colliculus. Neuroscience 160:103–114. https://doi.org/10.1016/j.neuroscience.2009.02.036
Mueller S, Wang D, Fox MD, et al (2013) Individual Variability in Functional Connectivity Architecture of the Human Brain. Neuron 77:586–595. https://doi.org/10.1016/j.neuron.2012.12.028
Nenning KH, Xu T, Schwartz E, et al (2020) Joint embedding: A scalable alignment to compare individuals in a connectivity space. Neuroimage 222:117232. https://doi.org/10.1016/j.neuroimage.2020.117232
Nichols T, Brett M, Andersson J, et al (2005) Valid conjunction inference with the minimum statistic. Neuroimage 25:653–660. https://doi.org/10.1016/j.neuroimage.2004.12.005
Nyffeler T, Kaufmann BC, Cazzoli D (2021) Visual Neglect After an Isolated Lesion of the Superior Colliculus. JAMA Neurol 78:1531–1533. https://doi.org/10.1001/jamaneurol.2021.3863
Patel GH, Yang D, Jamerson EC, et al (2015) Functional evolution of new and expanded attention networks in humans. Proc Natl Acad Sci 112:E5377–E5377. https://doi.org/10.1073/pnas.1516559112
Pedregosa F, Varoquaux G, Gramfort A, et al (2011) Scikit-learn: Machine Learning in Python. J Mach Learn Res 12:2825–2830. https://doi.org/10.1145/2786984.2786995
Petersen SE, Posner MI (2012) The attention system of the human brain: 20 years after. Annu Rev Neurosci 35:73–89. https://doi.org/10.1146/annurev-neuro-062111-150525
Posner MI (1980) Orienting of attention. Q J Exp Psychol 32:3–25. https://doi.org/10.1080/00335558008248231
Power JD, Cohen AL, Nelson SM, et al (2011) Functional network organization of the human brain. Neuron 72:665–678. https://doi.org/10.1016/j.neuron.2011.09.006.Functional
Prendergast MA, Jackson WJ, Terry Jr A V, et al (1998) Central nicotinic receptor agonists ABT-418, ABT-089, and (–)-nicotine reduce distractibility in adult monkeys. Psychopharmacol 136:50–58. https://doi.org/10.1007/s002130050538
Ptak R, Schnider A (2010) The dorsal attention network mediates orienting toward behaviorally relevant stimuli in spatial neglect. J Neurosci 30:12557–12565. https://doi.org/10.1523/JNEUROSCI.2722-10.2010
Ramsey LE, Siegel JS, Baldassarre A, et al (2016) Normalization of network connectivity in hemispatial neglect recovery. Ann Neurol 80:127–141. https://doi.org/10.1002/ana.24690
Repantis D, Schlattmann P, Laisney O, Heuser I (2010) Modafinil and methylphenidate for neuroenhancement in healthy individuals: A systematic review. Pharmacol Res 62:187–206. https://doi.org/10.1016/j.phrs.2010.04.002
Robinson EC, Jbabdi S, Glasser MF, et al (2014) MSM: A new flexible framework for Multimodal Surface Matching. Neuroimage 100:414–426. https://doi.org/10.1016/j.neuroimage.2014.05.069
Rolls ET, Huang CC, Lin CP, et al (2020) Automated anatomical labelling atlas 3. Neuroimage 206:. https://doi.org/10.1016/j.neuroimage.2019.116189
Saalmann YB, Kastner S (2011) Cognitive and Perceptual Functions of the Visual Thalamus. Neuron 71:209–223. https://doi.org/10.1016/j.neuron.2011.06.027
Sabuncu MR, Singer BD, Conroy B, et al (2010) Function-based intersubject

alignment of human cortical anatomy. Cereb Cortex 20:130–140. https://doi.org/10.1093/cercor/bhp085
Sanefuji M, Craig M, Parlatini V, et al (2017) Double-dissociation between the mechanism leading to impulsivity and inattention in Attention Deficit Hyperactivity Disorder: A resting-state functional connectivity study. Cortex 86:290–302. https://doi.org/10.1016/j.cortex.2016.06.005
Sani I, Stemmann H, Caron B, et al (2021) The human endogenous attentional control network includes a ventro-temporal cortical node. Nat Commun 12:1–16. https://doi.org/10.1038/s41467-020-20583-5
Schaefer A, Kong R, Gordon EM, et al (2018) Local-Global Parcellation of the Human Cerebral Cortex from Intrinsic Functional Connectivity MRI. Cereb Cortex 28:3095–3114. https://doi.org/10.1093/cercor/bhx179
Sheremata SL, Silver MA (2015) Hemisphere-dependent attentional modulation of human parietal visual field representations. J Neurosci 35:508–517. https://doi.org/10.1523/JNEUROSCI.2378-14.2015
Sherman SM (2007) The thalamus is more than just a relay. Curr Opin Neurobiol 17:417–422. https://doi.org/10.1016/j.conb.2007.07.003
Shu N, Liu Y, Li K, et al (2011) Diffusion tensor tractography reveals disrupted topological efficiency in white matter structural networks in multiple sclerosis. Cereb Cortex 21:2565–2577. https://doi.org/10.1093/cercor/bhr039
Shulman GL, Pope DLW, Astafiev S V., et al (2010) Right hemisphere dominance during spatial selective attention and target detection occurs outside the dorsal frontoparietal network. J Neurosci 30:3640–3651. https://doi.org/10.1523/JNEUROSCI.4085-09.2010
Snow JC, Mattingley JB (2006) Goal-driven selective attention in patients with right hemisphere lesions: How intact is the ipsilesional field? Brain 129:168–181. https://doi.org/10.1093/brain/awh690
Sprague JM (1966) Interaction of cortex and superior colliculus in mediation of visually guided behavior in the cat. Science (80-) 153:1544–1547. https://doi.org/10.1126/science.153.3743.1544
Stepniewska I, Kaas JH (1997) Architectonic subdivisions of the inferior pulvinar in New World and Old World monkeys. Vis Neurosci 14:1043–1060. https://doi.org/10.1017/s0952523800011767
Steriade M, Paré D, Parent A, Smith Y (1988) Projections of cholinergic and non-cholinergic neurons of the brainstem core to relay and associational thalamic nuclei in the cat and macaque monkey. Neuroscience 25:47–67. https://doi.org/10.1016/0306-4522(88)90006-1
Su JH, Thomas FT, Kasoff WS, et al (2019) Thalamus Optimized Multi Atlas Segmentation (THOMAS): fast, fully automated segmentation of thalamic nuclei from structural MRI. Neuroimage 194:272–282. https://doi.org/10.1016/j.neuroimage.2019.03.021
Suárez L, Markello R, Betzel R, Misic B (2020) Linking structure and function in macroscale brain. Trends Cogn Sci 24:302–315. https://doi.org/10.1016/j.tics.2020.01.008
Sun Y, Yang Y, Galvin VC, et al (2017) Nicotinic α4β2 cholinergic receptor influences on dorsolateral prefrontal cortical neuronal firing during a working memory task. J Neurosci 37:5366–5377. https://doi.org/10.1523/JNEUROSCI.0364-17.2017
Szczepanski SM, Konen CS, Kastner S (2010) Mechanisms of spatial attention control in frontal and parietal cortex. J Neurosci 30:148–160.

https://doi.org/10.1523/JNEUROSCI.3862-09.2010
Szczepanski SM, Pinsk MA, Douglas MM, et al (2013) Functional and structural architecture of the human dorsal frontoparietal attention network. Proc Natl Acad Sci U S A 110:15806–15811. https://doi.org/10.1073/pnas.1313903110
Thiebaut de Schotten M, Acqua FD, Forkel SJ, et al (2011a) A lateralized brain network for visuospatial attention. Nat Neurosci 14:1245–47. https://doi.org/10.1038/nn.2905
Thiebaut de Schotten M, ffytche DH, Bizzi A, et al (2011b) Atlasing location, asymmetry and inter-subject variability of white matter tracts in the human brain with MR diffusion tractography. Neuroimage 54:49–59. https://doi.org/10.1016/j.neuroimage.2010.07.055
Thiebaut de Schotten M, Foulon C, Nachev P (2020) Brain disconnections link structural connectivity with function and behaviour. Nat Commun 11:5094. https://doi.org/10.1038/s41467-020-18920-9
Thiebaut de Schotten M, Shallice T (2017) Identical, similar or different? Is a single brain model sufficient? Cortex 86:172–175. https://doi.org/10.1016/j.cortex.2016.12.002
Tournier JD, Smith R, Raffelt D, et al (2019) MRtrix3: A fast, flexible and open software framework for medical image processing and visualisation. Neuroimage 202:. https://doi.org/10.1016/j.neuroimage.2019.116137
Turner DC, Clark L, Dowson J, et al (2004) Modafinil improves cognition and response inhibition in adult attention-deficit/hyperactivity disorder. Biol Psychiatry 55:1031–1040. https://doi.org/10.1016/j.biopsych.2004.02.008
Uddin LQ, Yeo BTT, Spreng RN (2019) Towards a Universal Taxonomy of Macro-scale Functional Human Brain Networks. Brain Topogr 32:926–942. https://doi.org/10.1007/s10548-019-00744-6
Valentine G, Sofuoglu M (2017) Cognitive Effects of Nicotine: Recent Progress. Curr Neuropharmacol 16:403–414. https://doi.org/10.2174/1570159x15666171103152136
Valero-Cabré A, Toba MN, Hilgetag CC, Rushmore RJ (2020) Perturbation-driven paradoxical facilitation of visuo-spatial function: Revisiting the 'Sprague effect.' Cortex 122:10–39. https://doi.org/10.1016/j.cortex.2019.01.031
Van De Kar LD, Lorens SA (1979) Differential serotonergic innervation of individual hypothalamic nuclei and other forebrain regions by the dorsal and median midbrain raphe nuclei. Brain Res 162:45–54. https://doi.org/10.1016/0006-8993(79)90754-6
van den Heuvel MP, Sporns O (2013) Network hubs in the human brain. Trends Cogn Sci 17:683–696. https://doi.org/10.1016/j.tics.2013.09.012
Vazey EM, Moorman DE, Aston-Jones G (2018) Phasic locus coeruleus activity regulates cortical encoding of salience information. Proc Natl Acad Sci U S A 115:E9439–E9448. https://doi.org/10.1073/pnas.1803716115
Vergani F, Mahmood S, Morris CM, et al (2014) Intralobar fibres of the occipital lobe: A post mortem dissection study. Cortex 56:145–156. https://doi.org/10.1016/j.cortex.2014.03.002
Vossel S, Geng JJ, Fink GR (2014) Dorsal and ventral attention systems: Distinct neural circuits but collaborative roles. Neuroscientist 20:150–159. https://doi.org/10.1177/1073858413494269
Vossel S, Weidner R, Driver J, et al (2012) Deconstructing the architecture of dorsal and ventral attention systems with dynamic causal modeling. J Neurosci 32:10637–10648. https://doi.org/10.1523/JNEUROSCI.0414-12.2012

Vu AT, Auerbach E, Lenglet C, et al (2015) High resolution whole brain diffusion imaging at 7T for the Human Connectome Project. Neuroimage 122:318–331. https://doi.org/10.1016/j.neuroimage.2015.08.004

Vuilleumier P, Hester D, Assal G, Regli F (1996) Unilateral spatial neglect recovery after sequential strokes. Neurology 46:184–189. https://doi.org/10.1212/WNL.46.1.184

Washburn DA, Taglialatela LA (2006) Attention as it is manifest across species. In: Wasserman EA, Zentall TR (eds) Comparative cognition: Experimental explorations of animal intelligence. Oxford University Press, New York, pp 127–142

Wasserman EA, Castro L (2021) Assessing Attention in Category Learning by Animals. Curr Dir Psychol Sci 30:495–502. https://doi.org/10.1177/09637214211045686

Wassermann D, Makris N, Rathi Y, et al (2016) The white matter query language: a novel approach for describing human white matter anatomy. Brain Struct Funct 221:4705–4721. https://doi.org/10.1007/s00429-015-1179-4

Weddell RA (2004) Subcortical modulation of spatial attention including evidence that the Sprague effect extends to man. Brain Cogn 55:497–506. https://doi.org/10.1016/j.bandc.2004.02.075

Xu T, Nenning KH, Schwartz E, et al (2020) Cross-species functional alignment reveals evolutionary hierarchy within the connectome. Neuroimage 223:117346. https://doi.org/10.1016/j.neuroimage.2020.117346

Yeo BTT, Krienen FM, Sepulcre J, et al (2011) The organization of the human cerebral cortex estimated by intrinsic functional connectivity. J Neurophysiol 106:1125–1165

Zaborszky L, Hoemke L, Mohlberg H, et al (2008) Stereotaxic probabilistic maps of the magnocellular cell groups in human basal forebrain. Neuroimage 42:1127–1141. https://doi.org/10.1016/j.neuroimage.2008.05.055

Zénon A, Krauzlis RJ (2012) Attention deficits without cortical neuronal deficits. Nature 489:434–437. https://doi.org/10.1038/nature11497

Zhang F, Daducci A, He Y, et al (2022) Quantitative mapping of the brain's structural connectivity using diffusion MRI tractography: A review. Neuroimage 249:. https://doi.org/10.1016/j.neuroimage.2021.118870

Zoli M, Moretti M, Zanardi A, et al (2002) Identification of the nicotinic receptor subtypes expressed on dopaminergic terminals in the rat striatum. J Neurosci 22:8785–8789. https://doi.org/10.1523/jneurosci.22-20-08785.2002

Zolkowska D, Jain R, Rothman RB, et al (2009) Evidence for the involvement of dopamine transporters in behavioral stimulant effects of modafinil. J Pharmacol Exp Ther 329:738–746. https://doi.org/10.1124/jpet.108.146142